Visual Content Adaptation According to User Perception Characteristics

Jeho Nam, *Member, IEEE*, Yong Man Ro, *Senior Member, IEEE*, Youngsik Huh, and Munchurl Kim

***Abstract*—Adapting multimedia content to users' preferences and perceptual characteristics is a key direction for enabling personalized multimedia services. In this paper, we address the problem of tailoring visual content within the MPEG-21 Digital Item Adaptation (DIA) framework to meet users' visual perception characteristics. In particular, we present methods for adapting visual content to accommodate color vision deficiency and low-vision capabilities. In addition, we present methods for adapting visual content according to user preferences for color temperature. Finally, we report on experiments that adapt visual content within the MPEG-21 DIA framework.**

***Index Terms*—Accessibility, color temperature preference, color vision deficiency, Digital Item Adaptation (DIA), low vision, MPEG-21, personalizing, user characteristics.**

I. Introduction

MULTIMEDIA is becoming pervasive in our everyday life experiences. Transparent access to ubiquitous multimedia content needs to address multiple dimensions of the usage environment, including user characteristics, terminal capabilities, network characteristics and natural environment characteristics. User characteristics in particular have been identified as an important aspect of usage environment in previous work on Universal Multimedia Access (UMA) [1]–[3]. Personalized multimedia services have been drawing attention because of the growing capabilities and popularity of multimedia-enabled user devices (e.g., portable devices such as camera phones, audio-visual players, etc.). As a result, there has been growing research on content-based filtering and retrieval of multimedia resources. For example, Tseng *et al.* [4] and van Beek *et al.* [5] have each developed methods for exploiting users' content preferences for personalized browsing and multimedia summarization. The MPEG-7 standard (e.g., ISO/IEC 15938-5, Part 5 Multimedia Description Schemes) provides an important metadata framework for describing multimedia summaries and user preferences. As a result, there has been tremendous interest in building technologies for UMA based on the MPEG-7 standard [6].

Manuscript received May 7, 2004; revised January 24, 2005. The associate editor coordinating the review of this manuscript and approving it for publication was Dr. John R. Smith.

J. Nam is with the Electronics and Telecommunications Research Institute (ETRI), Daejeon 305-350, Korea (e-mail: namjeho@etri.re.kr).

Y. M. Ro and M. Kim are with the Multimedia Information Processing Group, Information and Communications University (ICU), Daejeon 305-714, Korea (e-mail: yro@icu.ac.kr; mkim@icu.ac.kr).

Y. Huh is with the Department of Mathematics, Hanyang Univesity, Seoul 133-791, Korea (e-mail: yshuh@hanyang.ac.kr).

Digital Object Identifier 10.1109/TMM.2005.846801

While MPEG-7 can be used to describe users' content preferences for personalized filtering, searching and browsing, MPEG-21 expands the scope to address seamless access of multimedia across devices, networks, and users. In particular, ISO/IEC 21000-7, MPEG-21 Part 7 "Digital Item Adaptation (DIA)," supports user-centric *adaptation* of multimedia content to the usage environment [7]. For example, MPEG-21 DIA addresses the customization of the *presentation* of multimedia content based on users' presentation preferences for content display/rendering, quality of service (QoS), and configuration and conversion with regard to multimedia modalities. In addition, MPEG-21 DIA supports user *accessibility* and personalization. For example, MPEG-21 DIA facilitates adaptation of multimedia resources according to the description of a user's audio-visual accessibility characteristics (e.g., audition and/or vision deficiencies).

The World Wide Web Consortium (W3C) has also addressed user access by developing a guideline for Web content developers (e.g., Web page authors and site designers) to support universal Web access. The document includes specific guidelines for visual accessibility [8]. However, the guideline focuses on HTML-based Web pages and falls short of more generally addressing access of image, video and multimedia content by the visually impaired. A few studies addressing reduced visual capabilities of users have been reported in the literature, but they provide only partial solutions [8]–[11]. In [9] and [10], color palettes were proposed for simulating the color perception of dichromats, who are affected by a partial color blindness in which only two colors are perceptible. However, the palettes are unavailable for anomalous trichromats. In [11], a heuristically obtained nonlinear filter was used to enhance color representation for anomalous trichromats on CRT monitors, but it is not practical in the general case because of reliance on specific properties of the display devices.

In this paper, we present visual content adaptation techniques considering the user's visual perception characteristics. First, we address how the visual properties of image and video content are adapted according to two types of visual accessibility characteristics: *color vision deficiency* and *low-vision impairment*. In particular, we propose novel approaches of modeling of and adaptation for anomalous trichromacy (a particular type of color vision deficiency) and for combined low-vision symptoms of "loss of fine detail" and "lack of contrast." In addition, user's preference on *color temperature* of image/video contents is discussed. Specifically, we present a scheme of how the temperature mapping between the original temperature and target temperature is determined by utilizing the MPEG-21 DIA color temperature preference descriptor.

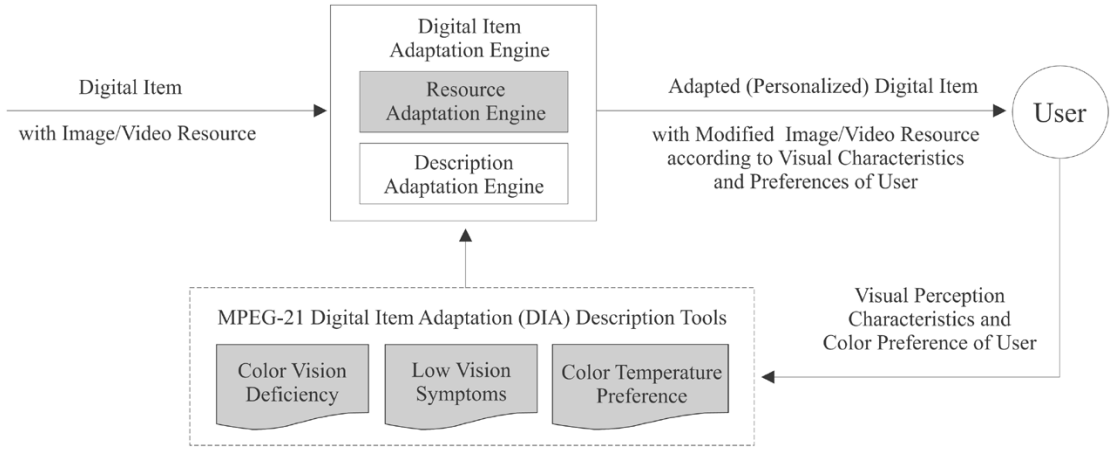

Fig. 1. MPEG-21 DIA according to visual perception characteristics of a user.

Fig. 1 illustrates the overview of our main contributions presented in this paper within the MPEG-21 DIA framework. The description tools in Fig. 1 are normative (standardized) parts of MPEG-21 DIA specification. It should be noted that in this paper we mainly focus on the technical aspects of the resource adaptation engine in Fig. 1, which is a nonnormative technology that supports the standard. We also describe the usage of the MPEG-21 DIA descriptors of color vision deficiency, low-vision symptoms and color temperature preferences, and provide examples. For details of normative syntax and semantics definition of the MPEG-21 DIA description tools, interested readers are referred to [7].

In Section II, visual accessibility of a user and associated content adaptation schemes are addressed. Color temperature preference is presented in Section III. Finally, experimental results and discussion are provided in Section IV and are followed by the conclusions.

II. Visual Accessibility

Access to text, image or video contents for visually deficient or impaired users may require methods for providing and controlling alternative selectable media presentation forms. For total blindness, it would be efficient to present audio information alone by providing alternative audio content or extracting audio stream only from a video clip, or by utilizing media modality conversion such as text-to-speech (TTS).

People with certain types of visual impairments have difficulty perceiving visual information. Nearsightedness, farsightedness, and distorted vision can often be corrected by appropriate glasses or medical procedures. However, severe *low vision* is not easily solved by these measures since it is often caused by complications from other diseases or circumstances. For example, the condition of *color vision deficiency* is most likely congenital and life long because no medical treatment is currently available.

In this section, we address visual content adaptation to accommodate color vision deficiency and low-vision impairment within MPEG-21 DIA framework.

A. Color Vision Deficiency

Color vision deficiency generally arises from two causes: 1) complete lack or 2) modification of one of three classes of cone pigments. The former is called *dichromacy* and the latter is called *anomalous trichromacy*. There is also an extreme case, called *achromatopsia*, where the visual system is altogether lacking cones and the ability to perceive color [12].

In the case of dichromacy, entire colors in visible spectrum are seen with two monochromatic hues. Anomalous trichromacy, which arises from a variety of causes, results in color distortion. Anomalous trichromacy is the most common color vision deficiency, comprising more than 80% of the cases of color vision deficiency [12]. According to research in molecular genetics, the most common cause of anomalous trichromacy is believed to be a shift of the peak sensitivity of a cone [13]–[15]. In anomalous trichromacy, the peak sensitive wavelengths of two classes are closer than normal trichromat in three classes of cone pigments. This causes different sensitivity of colors and thereby colors are confused. The visible color range is reduced due to two closer peak sensitivities. The deficiency degree is dependent on the distance from two peak sensitive wavelengths. Anomalous trichromacy is categorized into three types according to abnormal cone; *protanomaly* caused by an abnormal L (long wavelength) cone, *deuteranomaly* caused by an abnormal M (middle wavelength) cone, and *trianomaly* caused by an abnormal S (short wavelength) cone. It results in the degraded differential sensitivity of color and the confused color, e.g., the visible color range of anomalous trichromat becomes reduced compared with normal trichromat. Fig. 2 shows a simulation of what color images look like to people with dichromacy and anomalous trichromacy.

To address color vision deficiency, MPEG-21 DIA has developed a description tool called `ColorVisionDeficiency` in which the type of deficiency and its degree of severity are described both qualitatively and quantitatively. This is necessary, for example, since dichromacy has one degree of severity while anomalous trichromacy is represented by a numerical degree in a range of 0.0–0.9 of severity at each type. Fig. 3 shows an instance of the MPEG-21 DIA `ColorVisionDeficiency` that describes color vision deficiency characteristics of a user who

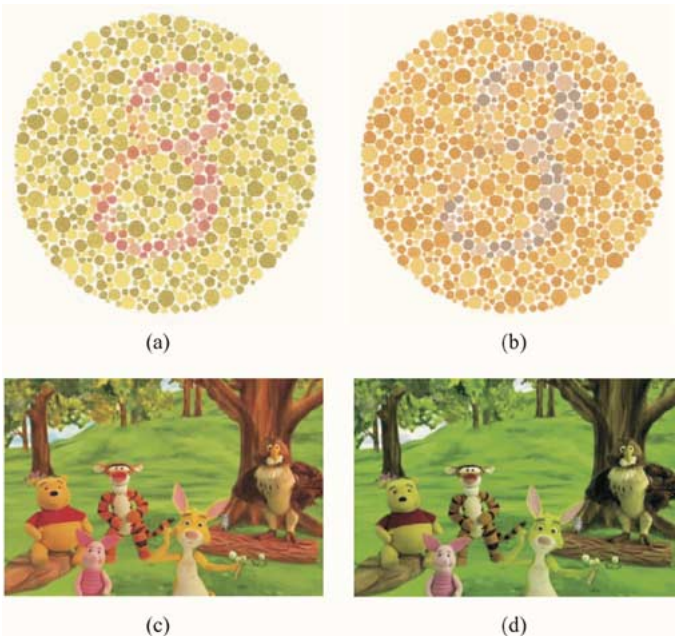

Fig. 2. Color vision deficiency: (a) original Ishihara image; (b) simulated (dichromacy) image of (a); (c) original animation image; and (d) simulated (anomalous trichromacy) image of (c).

has a certain type and degree of color vision deficiency, e.g., mild red-color deficiency (protanomaly).

In Fig. 3, the numerical degree can be measured by taking into account both the severity in the Hardy-Rand-Ritter (HRR) test [16] and the total error score in Farnsworth-Munsell (FM)-100 hue test [17]. The total error score is a measured score defined in the FM-100 hue test. In this paper, the deficiency degree was obtained by linearly quantizing the total error score values with the lower and upper limits of the total error score in FM-100 hue test.

Visual information of multimedia content is seen through a display device of a terminal. Since the display device has its own spectral emission characteristics, users perceive the color with the display characteristics as well. In protanomaly, the spectral response of L cone for individual primary phosphor (R, G, B) is defected as [18]

$$\begin{aligned} L_R^{\text{abnormal}}\big|_n &= k_L \int R(\lambda)L(\lambda - \Delta d(n))d\lambda \\ L_G^{\text{abnormal}}\big|_n &= k_L \int G(\lambda)L(\lambda - \Delta d(n))d\lambda \\ L_B^{\text{abnormal}}\big|_n &= k_L \int B(\lambda)L(\lambda - \Delta d(n))d\lambda \end{aligned} \tag{1}$$

where n is the deficiency degree of anomalous trichromacy, $\Delta d(n)$ is the shifted amount of the abnormal cone peak sensitivity about the deficiency degree n, and $R(\lambda)$, $G(\lambda)$, and $B(\lambda)$ are the spectral emission functions of each phosphor over wavelength λ. In general, the function $\Delta d(n)$ can be obtained by analyzing abnormal genes studied in molecular genetics [12], [14], [15]. In this paper, we simply characterize the function $\Delta d(n)$ by a linear quantization of degree n, within a range of minimum and maximum bounds [12] of corresponding shifted amount of abnormal cone peaks at each deficiency type. Specifically, the function $\Delta d(n)$ can be written as $\Delta d(n) = \text{nint}\left[\left(\lambda_{\max}^{\text{shift}} - \lambda_{\min}^{\text{shift}}\right) n\right]$, where the function $\text{nint}[\cdot]$ is to take the nearest integer value.

```
<?xml version="1.0" encoding="UTF-8"?>
<DIA xmlns="urn:mpeg:mpeg21:2003:01-DIA-NS"...>
  <Description xsi:type="UsageEnvironmentType">
    <UsageEnvironmentProperty xsi:type="UsersType">
      <User>
        <UserCharacteristic xsi:type="VisualImpairmentType">
          <ColorVisionDeficiency>
            <DeficiencyType>Red-Deficiency</DeficiencyType>
            <DeficiencyDegree>
              <NumericDegree>0.5</NumericDegree>
            </DeficiencyDegree>
          </ColorVisionDeficiency>
        </UserCharacteristic>
      </User>
    </UsageEnvironmentProperty>
  </Description>
</DIA>
```

Fig. 3. Example of a MPEG-21 DIA color vision deficiency description.

It is assumed that the display device has an ideal emission function so that the neutral LMS response is purely white point. Given this condition, the parameters of k_L are computed as values satisfy $\Sigma L = \Sigma M = \Sigma S = 1$. Similarly, the spectral responses of M cone in deuteranomaly and the spectral responses of S cone in tritanomaly are obtained [19].

With the spectral responses of defected L cone, abnormal LMS cone responses of a protanomaly are written as

$$\begin{bmatrix} L^{\text{abnormal}} \\ M^{\text{normal}} \\ S^{\text{normal}} \end{bmatrix} = \mathbf{T}_L^{\text{abnormal}} \cdot \begin{bmatrix} R \\ G \\ B \end{bmatrix} \tag{2}$$

$$\mathbf{T}_L^{\text{abnormal}} = \begin{bmatrix} L_R^{\text{abnormal}} & L_G^{\text{abnormal}} & L_B^{\text{abnormal}} \\ M_R^{\text{normal}} & M_G^{\text{normal}} & M_B^{\text{normal}} \\ S_R^{\text{normal}} & S_G^{\text{normal}} & S_B^{\text{normal}} \end{bmatrix} \tag{3}$$

where the conversion matrix $\mathbf{T}_L^{\text{abnormal}}$ maps colors in RGB space into defected ones by abnormal LMS cone. Similarly, the conversion matrices for the deuteranomaly and the tritanomaly, which are denoted as $\mathbf{T}_M^{\text{abnormal}}$ and $\mathbf{T}_S^{\text{abnormal}}$ respectively, can be obtained [19].

As mentioned above, the characteristics of color vision deficiency and display device should be measured as parameters for content adaptation. Given these parameters, we first consider how the anomalous trichromat perceives the colors emitted from the display device [20]. In case of protanomaly, a RGB color (R, G, B) is defected into $\left(R_L^{\text{defected}}, G_L^{\text{defected}}, B_L^{\text{defected}}\right)$ as follows [18]:

$$\begin{bmatrix} R_L^{\text{defected}} \\ G_L^{\text{defected}} \\ B_L^{\text{defected}} \end{bmatrix} = \left[\mathbf{T}^{\text{normal}}\right]^{-1} \cdot \begin{bmatrix} L^{\text{abnormal}} \\ M^{\text{normal}} \\ S^{\text{normal}} \end{bmatrix}. \tag{4}$$

Note that the $\mathbf{T}^{\text{normal}}$ is a conversion matrix for normal user, i.e., conversion from RGB space into normal LMS space. Similarly, the RGB color is defected into $\left(R_M^{\text{defected}}, G_M^{\text{defected}}, B_M^{\text{defected}}\right)$ in deuteranomaly and $\left(R_S^{\text{defected}}, G_S^{\text{defected}}, B_S^{\text{defected}}\right)$ in tritanomaly, respectively.

Note that the goal of the content adaptation is to compensate anomalous trichromat for defected color information. The content adaptation is performed to make the defected color $\left(R_S^{\text{defected}}, G_S^{\text{defected}}, B_S^{\text{defected}}\right)$ be equal to the original color (R, G, B) in viewpoint of anomalous trichromacy.

Thus, the adapted stimulus $\left(R^{\text{adapted}}, G^{\text{adapted}}, B^{\text{adapted}}\right)$ can be simply induced by inverse matrix operation as follows:

$$\begin{bmatrix} R^{\text{adapted}} \\ G^{\text{adapted}} \\ B^{\text{adapted}} \end{bmatrix} = \left[\mathbf{T}^{\text{abnormal}}\right]^{-1} \cdot \left[\mathbf{T}^{\text{normal}}\right] \cdot \begin{bmatrix} R \\ G \\ B \end{bmatrix}. \quad (5)$$

By using (5), one can obtain the adapted color according to one's color deficiency degree of one's MPEG-21 color vision deficiency description. Note that the matrix $\mathbf{T}$ is always invertible because all three sensitivities of three orthogonal cones (L, M, S) have nonzero values, so that the $\mathbf{T}$ has a nonzero determinant. In Section IV, we present experimental results with the subjects of anomalous trichromat.

B. Low-Vision Impairment

Low vision is usually caused by eye diseases and health conditions such as cataract, diabetes, macular degeneration and glaucoma etc [21]. Unfortunately, it is difficult to correct by glasses or medical treatment. Most types of low-vision impairment have a limited set of common symptoms [22], [23]. Some of these symptoms happen occasionally to people with normal vision when they suffer from temporary eye diseases.

To describe the type and degree of low-vision impairment, the MPEG-21 DIA standard supports "symptom" based description, rather than individually identified names of eye diseases. Typical symptoms caused by various low-vision impairments are summarized as follows.

- *Loss of fine detail:* this symptom causes the perceived image blurred; it can be described by the normal visual acuity measurement,
- *Lack of contrast:* this symptom causes the dynamic range of image intensity to be reduced; it can be described by the contrast sensitivity measurement,
- *Light sensitivity:* this symptom, also called photophobia, describes the user's extreme light sensitivity to the normal light condition,
- *Need of light:* this symptom causes the patient to perceive the image with a lower brightness than it should be,
- *Central vision loss:* this symptom describes the loss at the center of vision field (e.g., black "patch"),
- *Peripheral vision loss:* this symptom describes the loss at the periphery of the vision field (e.g., "tunnel effect")

In the MPEG-21 DIA `LowVisionSymptoms` description tool, the degree of symptoms is represented by a numeric value in a range of 0.0–1.0. The higher the level is, the more severe the symptom becomes. The value of 0.0 means no symptom, while the value of 1.0 means the total disability due to that symptom. The severity level of these symptoms could be also given subjectively in a categorized degree (mild, medium, severe) without a specific numeric value (when the numeric degree is not available), and the system can select a certain adaptation scheme for each categorized degree. Fig. 4 shows an instance of the MPEG-21 DIA `LowVisionSymptoms` description in which the type and degree of low-vision symptom are provided.

It is possible that a user may give the degree in the specific format of a symptom measurement. For example, the symptom of "loss of fine detail" can be described by familiar visual acuity measurement ranged from 20/20 to 0/20. Then that specific degree will be inversely mapped into the range of 0.0–1.0 (as a numeric value of the MPEG-21 DIA descriptor). Given the list of symptoms and the associated degrees, we can have the essential information to model the vision system of the user.

```
<?xml version="1.0" encoding="UTF-8"?>
<DIA xmlns="urn:mpeg:mpeg21:2003:01-DIA-NS" ...>
  <Description xsi:type="UsageEnvironmentType">
    <UsageEnvironmentProperty xsi:type="UsersType">
      <User>
        <UserCharacteristic xsi:type="VisualImpairmentType">
          <LowVisionSymptoms>
            <LossOfFineDetail>
              <TextualDegree>Mild</TextualDegree>
            </LossOfFineDetail>
            <LackOfContrast>
              <TextualDegree>Severe</TextualDegree>
            </LackOfContrast>
            <CenterVisionLoss>
              <NumericDegree>0.5</NumericDegree>
            </CenterVisionLoss>
          </LowVisionSymptoms>
        </UserCharacteristic>
      </User>
    </UsageEnvironmentProperty>
  </Description>
</DIA>
```

Fig. 4. Example of a MPEG-21 low-vision impairment description.

The difficulties of the low-vision users can be ameliorated by image enhancement and adaptation techniques [24]. Actually, the current state of study on human visual system (HVS) in the literature is not mature enough to incorporate all the above symptoms in a HVS model. The loss of fine detail and lack of contrast, corresponding to visual acuity and contrast sensitivity measurements in medical practice, are the two most popular symptoms and profoundly studied so far. Other symptoms are still being investigated. Therefore, in this paper we currently focus on the first two symptoms: "loss of fine detail" (denoted by L_d) and "lack of contrast" (denoted by L_c).

Our contribution on low vision in this paper is to build an HVS model incorporating these two symptoms. In particular, the symptoms are employed to model the human visual characteristics. Given the model, the MPEG-21 DIA based content adaptation can be carried out accordingly. As mentioned above, L_d can be obtained from the visual acuity test and L_c from the contrast sensitivity test, and then normalized into a range of $[0, 1]$ which can be represented in the MPEG-21 DIA `LowVisionSymptoms` descriptor.

For each user, these parameters L_d and L_c are used to constitute an analytical contrast sensitivity function (CSF) [25] that shows the user's contrast sensitivity with respect to spatial frequency. Denote the CSF of a normal user by $CSF(f)$, where f is the spatial frequency measured in cycles/degree. We can note that the clinical contrast sensitivity reflects the contrast sensitivity near the peak of the function and clinical visual acuity reflects the sensitivity at the right-hand limit of the function. We observe that when L_c increases, the function is scaled down; and when L_d increases, the function is shrunk. So, we construct the contrast sensitivity function of a low-vision user, $CSF_{lv}(f)$, as follows:

$$CSF_{lv}(f) = (1 - L_c) \cdot CSF\left(\frac{f}{1 - L_d}\right). \quad (6)$$

Here, we combine the analytical CSF of a normal user from [26] with our proposed construction in (6), then we now obtain

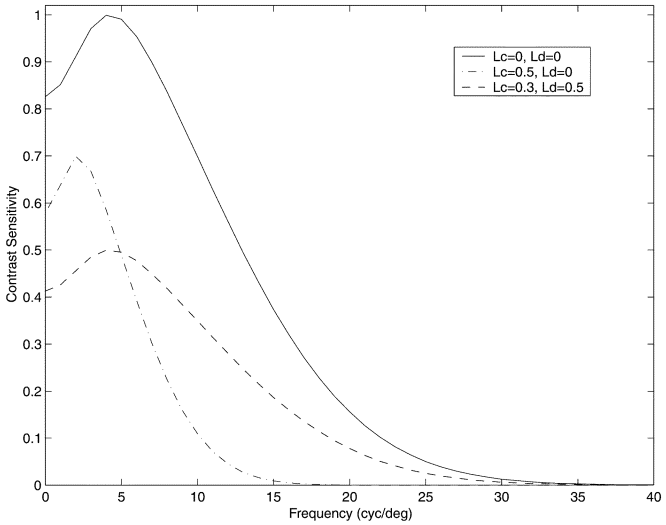

Fig. 5. Illustration of different contrast sensitivity functions (CSF_{lv}) for different cases of L_d and L_c.

the $CSF_{lv}(f)$ for low-vision user as follows:

$$CSF_{lv}(f) = (1 - L_c) \cdot 2.93 \cdot \left[0.393 \cdot e^{-(\pi \cdot 0.393 \cdot f \cdot 0.075/(1-L_d))^2} - 0.063 \cdot 1.768 \cdot e^{-(\pi \cdot 1.768 \cdot f \cdot 0.075)/(1-L_d)^2}\right]. \quad (7)$$

With this modified CSF for a low-vision user, we can see that when L_c increases, the $CSF_{lv}(f)$ will be scaled down, causing the contrast sensitivity over the whole range of frequency to be reduced. Similarly, when L_d increases, the $CSF_{lv}(f)$ will be shrunk, reducing the sensitivity over the high-frequency range. Some examples of the $CSF_{lv}(f)$ over different degrees of L_c and L_d are illustrated in Fig. 5.

As for adaptation for low-vision symptoms modeled by (7), we extend the method of [27] that adapts the visual content according to user's characteristics and content characteristics. The local characteristics (frequency and contrast) of visual content is checked and the local contrast is increased accordingly to these characteristics so as the content is enhanced while undistorted at the same time. Recall that the normal $CSF(f)$ in [27] should be replaced by the low-vision $CSF_{lv}(f)$ described by (7).

To incorporate other low-vision symptoms, we may need to employ more complex models. Ferwerda [28] has presented some models for tone reproduction in image rendering. These models can be applied to handle the symptoms such as "need of light" and "light sensitivity". Table I provides possible content adaptation schemes that are effective solutions to the symptoms of low vision.

Contrast control (enhancement) is obviously useful to improve the visibility in most cases, especially when the user has lack of contrast and loss of fine detail. Sharpness enhancement also helps the user with loss of fine detail to see more clearly the remaining details (e.g., major edges in images) in the visible range of the user. Brightness control would be the main tool to help the user with light sensitivity or need of light. In some cases, the increase of brightness is also effective to other symptoms because the user would have better intensity level discrimination when the brightness is increased. Glaring phenomenon is very annoying to users having light sensitivity. This problem is normally solved by some nonlinear manipulation on pixel intensities, which we call glare control.

TABLE I
POSSIBLE ADAPTATION SCHEMES TO COMPENSATE THE LOW VISION

	contrast control	sharpness control	brightness control	glare reduction	size change
Lack of fine detail	**	**	*		**
Lack of contrast	**	*	*		**
Light sensitivity	*	*	**	**	*
Need of light	*		**		*
Partial loss of vision field	*	*	*		**

* indicates the priorities of corresponding approaches. Problem of multiple symptoms needs combined approaches.

Size control, specifically enlargement, will reduce the spatial frequency spectrum of images, i.e., more details become visible through the lowpass-like vision system of users with loss of fine detail and lack of contrast. Also, size increase (or reduction) is the first choice to bring more details to the limited vision field of users with symptoms related to partial loss of vision field. With central vision loss, the image would be enlarged and vice versa with peripheral vision loss, the image would be downscaled. It should be noted that the *modality conversion* (e.g., media conversion from text/image/video to audio/Braille) can be effectively applied to any of low-vision impairments as well as the blindness, but visual information is no longer available.

III. COLOR TEMPERATURE PREFERENCE

In this section, we address the utilization of *color temperature* preference of a user, within the MPEG-21 DIA framework. Color temperature is defined as the correlated temperature of estimated illumination of color images, and it relates to the energy of illumination in the image [29], [30]. The preferred color temperature is quite dependent on each person's taste. If the color temperature is low, an image looks reddish (precisely, the image looks as if it was taken under reddish illumination). Whereas, the image looks bluish if the color temperature is high. The feature values of the color temperature (e.g., in MPEG-7 descriptor) can be extracted by calculating the correlated color temperature of luminous pixels [30]–[32].

The necessary steps of color temperature adaptation within the MPEG-21 DIA framework can be summarized as follows:

1) obtaining color temperature preferences from a user;
2) estimating color temperature from input image;
3) determining target color temperature from preference information (equivalently, determining a temperature mapping function);
4) transforming pixel values of the original (input) image so that the converted image has the intended target color temperature.

Here, the target temperature means the expected color temperature that the output image should have. Fig. 6 depicts the

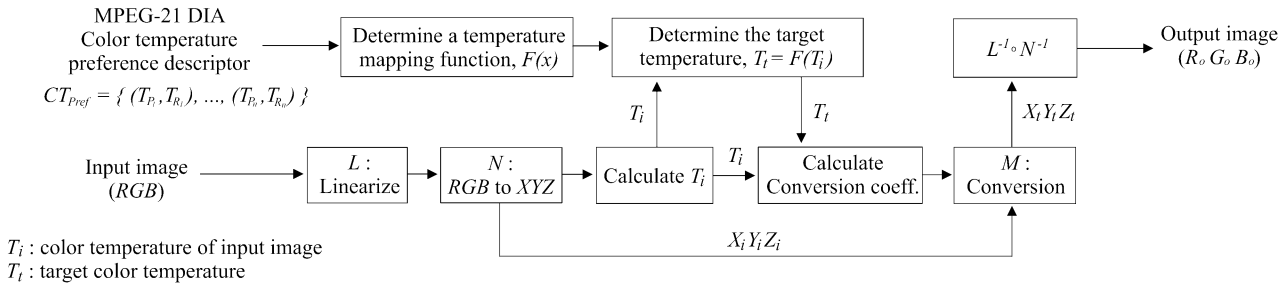

Fig. 6. Flow diagram of color temperature conversion.

flow diagram of color temperature adaptation in the context of MPEG-21 DIA. Note that the details of the steps 2) and 4) have been addressed in [31], [32] in the context of MPEG-7 standard technologies.

In the rest of this section, we mainly focus on the technical aspects of the step 1) and 3) above. First, we briefly describe of how to obtain color temperature preferences from a user and represent it into the MPEG-21 DIA descriptor, with regard to the step 1). Then, we specify the issue of the step 3). Particularly, we propose several conditions that a temperature mapping function should satisfy and discuss how the preference data should be utilized to select a proper mapping function.

To obtain the preferred color temperature of a user, we generate a set of images with the same content but various color temperature values. These images of different temperature version and the original image are shown to a user and the user is asked to select the most preferred image in comparison with the original. If the color temperatures of the original image and the selected image are denoted by T_R and T_P respectively, then the preference descriptor is set to be $\{(T_P, T_R)\}$. This guides how the color attribute of a displayed image should be controlled, so that the perceived color conforms to the temperature preference of a user. For instance, $CT_{\mathrm{Pref}} = \{(T_P, T_R)\}$ means that a user wants to convert an image of color temperature T_R into an image of color temperature T_P.

If n sets of test images are shown, the preference descriptor would be a form of $\{(T_{P_1}, T_{R_1}), \ldots, (T_{P_n}, T_{R_n})\}$, which describes user's preference more precisely than the descriptor with only one pair of values. The proper number of test set is dependent on each specific application. Fig. 7 shows an instance of the MPEG-21 DIA `ColorTemperaturePreference` description in which the color temperature preference is provided by $\{(78, 100), (160, 178), (208, 185), (227, 205)\}$.

Now, we deal with the issue of the step 3). The determination of a target temperature is to formulate a *temperature mapping* function $F(x)$, in which the input is the color temperature T_i of the input image and the output is the target temperature T_t, as shown in Fig. 6. To guarantee that the converted image looks natural, it is desirable that the mapping function $F(x)$ satisfies the following conditions.

1) If $x_1 < x_2$, then $F(x_1) < F(x_2)$.
2) $F(x)$ is smooth (or differentiable).
3) $F(0) = 0$ and $F(1) = 1$ (assuming the range of feature values is normalized into $[0, 1]$).

Note that the condition 1) guarantees the consistency of color temperature conversion and the condition 2) is required especially when a sequence of images (e.g., video) is presented continuously to a user. The condition 3) ensures that the range of color expression is not reduced. Therefore, the determination of the temperature mapping function $F(x)$ is to find a smooth increasing function that approximates the finite discrete points, $\{(T_{P_i}, T_{R_i}) \mid i = 1, \ldots, n\}$, such that $F(T_{R_i}) \approx T_{P_i}$.

```
<?xml version="1.0" encoding="UTF-8"?>
<DIA xmlns="urn:mpeg:mpeg21:2003:01-DIA-NS"...>
   <Description xsi:type="UsageEnvironmentType">
      <UsageEnvironmentProperty xsi:type="UsersType">
         <User>
            <UserCharacteristic
                xsi:type="DisplayPresentationPreferencesType">
               <ColorTemperaturePreference>
                  <BinNumber>255</BinNumber>
                  <Value>
                     <PreferredValue>78</PreferredValue>
                     <ReferenceValue>100</ReferenceValue>
                  </Value>
                  <Value>
                     <PreferredValue>160</PreferredValue>
                     <ReferenceValue>178</ReferenceValue>
                  </Value>
                  <Value>
                     <PreferredValue>208</PreferredValue>
                     <ReferenceValue>185</ReferenceValue>
                  </Value>
                  <Value>
                     <PreferredValue>227</PreferredValue>
                     <ReferenceValue>205</ReferenceValue>
                  </Value>
               </ColorTemperaturePreference>
            </UserCharacteristic>
         </User>
      </UsageEnvironmentProperty>
   </Description>
</DIA>
```

Fig. 7. Example of a MPEG-21 DIA color temperature preference description.

A difficulty may happen when the number of preference data is very small, because we have too much freedom of approximation. Furthermore, when the approximated function has many points of inflection on which the curve shape of $F(x)$ is changed, the converted image sequence may look unnatural. So, in this case, it would be safe to use a function with least number of inflection points, rather than to attempt to find a function approximating the preference data completely. For this kind of approach, it needs to analyze the distribution of preference data and then to induce the rough patterns of preference. Possible interpretation can be one of the following:

1) user prefers higher color temperatures:
   $T_{P_i} > T_{R_i}$ for almost all i;
2) user prefers lower color temperatures:
   $T_{P_i} < T_{R_i}$ for almost all i;
3) user wants to emphasize the difference of color temperatures:
   for $T_{R_i} \ll T_{R_j}$, $T_{P_i} < T_{R_i}$ and $T_{P_j} > T_{R_j}$.

In cases of 1) and 2) above, a gamma function, i.e., a form of $(Ax + B)^{\gamma}/N + C$, can be a candidate for $F(x)$ because it satisfies all of the required conditions for mapping function and has no inflection point. In case of 3), we can use a sigmoidal

function, i.e., a form of $1/(1+Ae^{Dx+E})$, which has only one inflective (but differentiable) point.

One extreme case is that the CT_{Pref} has only one pair of color temperature values, $\{(T_P, T_R)\}$. Also in this case, a gamma function can be selected. Another candidate is a linear function as follows:

$$F(x) = \begin{cases} \frac{(T_{\max}-T_P)(x-T_R)}{(T_{\max}-T_R)} + T_P, & \text{if } x > T_R, \\ \frac{(T_P-T_{\min})(x-T_{\min})}{(T_R-T_{\min})} + T_{\min}, & \text{otherwise} \end{cases} \quad (8)$$

where x denotes the color temperature of an input image. If the temperatures are expressed in MPEG-7 color temperature descriptor, then $T_{\max}$ and $T_{\min}$ should be 255 and 0, respectively. Although the linear temperature mapping in (8) is simply obtained, it may not be smooth enough at T_R. In order to make up this defect, a mapping function that is composed of power functions and linear functions was proposed in [33].

Note that the screen size of a display and the depth of color are factors to be considered in the determination of a mapping function. If a display device has a small screen and low color depth (e.g., PDA), the precision and smoothness are not much important. Thus, a linear mapping in (8) would be enough.

Recall that after the temperature mapping function $F(x)$ and the color temperature T_i of the input image are obtained, the target temperature T_t should be determined by $T_t = F(T_i)$ as shown in Fig. 6. From T_t and T_i, the conversion coefficients are computed. The conversion coefficients constitute a linear mapping M that sends (X_i, Y_i, Z_i) to (X_t, Y_t, Z_t). Here, (X_i, Y_i, Z_i) denotes a pixel value of the input image in CIE 1931 tristimulus space and (X_t, Y_t, Z_t) are the pixel value of the converted image. A detailed explanation of how to calculate the conversion coefficients and linear mapping M is addressed in [32] and [33], where the ratio of two tristimulus values determines the coefficients through the Bradford chromatic adaptation transformation [30], [34].

Finally, we obtain the RGB pixel values of the output image (i.e., converted image based on user's preferred color temperature) by

$$(R_o, G_o, B_o) = (L^{-1} \circ N^{-1} \circ M \circ N \circ L)(R, G, B) \quad (9)$$

where the $\circ$ denotes the composition of two mapping such as $f(x) \circ g(x) = f(g(x))$, L is a nonlinear function that linearizes the input (R, G, B) and N is a linear transform from RGB space to the CIE 1931 tristimulus XYZ space.

IV. Experiments

Experiments are performed to verify the proposed visual content adaptation schemes in accordance with MPEG-21 DIA descriptors. In particular, we present experimental results with our proposed modeling and adaptation methods for anomalous trichromacy, and for combined low-vision symptoms (i.e., modified contrast sensitivity function for low vision), and with color temperature mapping and thereby adaptation scheme with user's preferred color temperature, which are all addressed in the previous sections.

For color vision deficiency, test data consists of a total of ten images that includes natural photos and presentation material (e.g., graphical charts). The test images are selected from the data set used in MPEG-21 DIA core experiment [35]. As a display device, Samsung SM 950+ CRT monitor was used. The spectral emission function of the display device was measured by spectroradiometer (Minolta CS-1000).

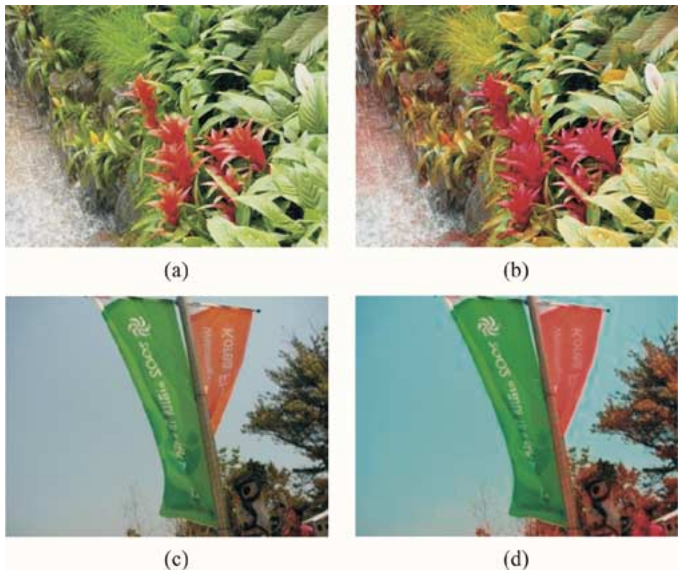

Fig. 8. Color vision deficiency (deuteranomaly): (a) original image of a flower; (b) color adapted image of (a); (c) original image of a banner; and (d) color adapted image of (c).

TABLE II
Comparison of Detection Result on Test Data Set

ID (age)	HRR test	Computerized FM-100 hue test[a]	MPEG-21 DIA
	severity	total error score (left/right eye)	numerical degree
1 (20)	strong	244/188	0.9
2 (37)	medium	172/208	0.6
3 (34)	medium	240/224	0.6
4 (22)	mild	192/56	0.3

[a]Seohan color vision test [36]

We performed a clinical test with four subjects who have color vision deficiency of deuteranomaly. They had carried out all three color vision tests: 1) Ishihara test; 2) HRR test [16]; and 3) Seohan color vision test [36]. The last one is very similar to a computerized Farnsworth-Munsell (FM) test [17]. Performance was evaluated by subjective responses from each of the subjects. With the subjects, we adapted colors on the test images and then displayed two images side-by-side; the original image and its color-adapted version. Fig. 8 shows examples of the test images used in our experiment. Original color photo images of a flower and a banner are shown in Fig. 8(a) and (c), respectively. Their color adapted versions for deuteranomaly are shown in Fig. 8(b) and (d), respectively.

Recall that the color adaptation is performed in accordance with deficiency type and degree; both values are provided by the MPEG-21 DIA descriptor. For the deficiency degree, we applied 0.3 for mild severity, 0.6 for medium severity, and 0.9 for strong severity. Table II shows that mappings between the color vision tests and MPEG-21 DIA description. In a current preliminary experiment, we had four subjects who were one mild, two medium, and one strong color deficiency. The severity was

TABLE III
RESULTS OF SUBJECTIVE RESPONSE FROM COLOR VISION DEFICIENCY

ID (age)	better	equal	worse
1 (20)	7	1	2
2 (37)	8	1	1
3 (34)	8	0	2
4 (22)	2	8	0
total number of responses	35		5
average number of responses	8.75		1.25

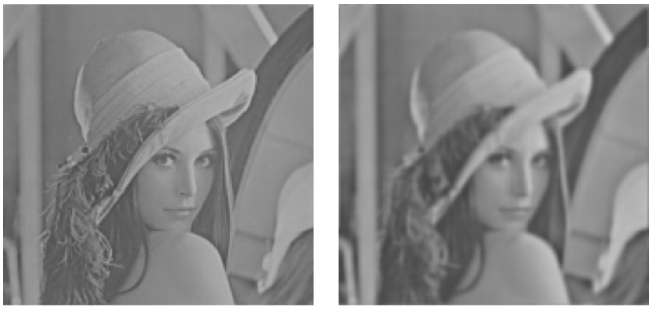

(a) (b)

Fig. 9. Simulated images of combined symptom model. (a) $L_c = 0.5$ and $L_d = 0$. (b) $L_c = 0.3$ and $L_d = 0.7$.

measured by the HRR test. For the third volunteer $(\mathrm{ID} = 3)$, the HRR test and FM-100 test results were not coincident as seen in the Table II. Because of a few data in this preliminary experiment, we did not obtain the numerical degree using linear quantization of total error score in FM-100. But, we assigned numerical degree by the HRR test in this experiment.

Next, the subjects were asked with some questionnaires, which inquired the subjects about some confusing area in the images. For simple evaluation, we limited the subject's response to be one of "better", "equal", or "worse". The "better" case shows that a color-confused region is more clearly discernable in the adapted image than in the original image. The "worse" case shows that a color-confused region is less discernable in the adapted image than in the original image, and the "equal" case shows that the subject's color discrimination is not quite different from each other.

Table III shows the result of subjective responses on a total of ten test images. The subjects responded "better" or "equal" in 8.75 of the ten images on average. On the other hand, they responded "worse" in only 1.25 images, on average. These show that the proposed color adaptation technique provides better or equal visual accessibility to color-deficient users (anomalous trichromat).

As for experiments with low-vision impairment, we first apply our proposed symptom model (i.e., modified contrast sensitivity function for low vision) in (7) to test the different adaptation techniques that cope with the loss of fine detail and the lack of contrast. Fig. 9 shows the simulated images for different degrees of two symptoms (L_c and L_d) that are provided by the MPEG-21 DIA descriptor.

For our low-vision adaptation, we find that the pre-emphasis technique in [24] is not effective for Lenna image in particular as well as for many other images in general. This is because the images are usually sharp already and the pre-emphasizing would rather cause artifact or distortion to the original images. From our experiment, we also find the adaptive contrast enhancement in [27] (e.g., some heuristic contrast stretching) gives better visibility to the low-vision user. Fig. 10 shows the results of image adaptation that is based on contrast stretching for low-vision symptoms with $L_d = 0.9$. Fig. 11 shows the results of image adaptation that is for combined low-vision symptoms with of "loss of fine detail" $(L_d = 0.1)$ and "lack of con-

(a) (b) (c) (d)

Fig. 10. Adaptation (contrast stretching) for the "loss of fine detail" symptom: (a) original image; (b) simulated image with $L_d = 0.9$; (c) adapted image; and (d) simulated image $(L_d = 0.9)$ of adapted image (c).

(a) (b) (c) (d)

Fig. 11. Adaptation for combined symptoms of "loss of fine detail" and "lack of contrast": (a) original image; (b) simulated image with $L_d = 0.1$ and $L_c = 0.9$; (c) adapted image; and (d) simulated image ($L_d = 0.1$ and $L_c = 0.9$) of adapted image (c).

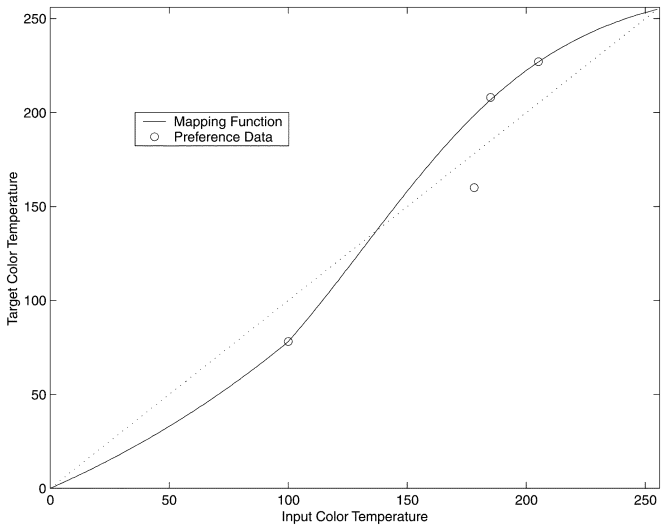

Fig. 12. Curve fitting of preference data.

trast" $(L_c = 0.9)$. As shown in Figs. 10 and 11, visual contents in adapted images, Figs. 10(d) and 11(d), look more discernable (i.e., visually enhanced), compared with their corresponding visually impaired images, Figs. 10(b) and 11(b), respectively.

Some simple adaptation schemes can be applied for the losses of vision field. It is obvious that the most appropriate adaptation method for these kinds of symptoms (center vision loss and peripheral vision loss) is adjustment of image sizes. For example, with the loss of the center vision field, the image size should be enlarged. Of course, the low-vision users having these symptoms can change the vision field themselves by adjusting the viewing direction. However, when the viewing direction and viewing distance are fixed (e.g., user of a wearable TV), this simple and yet effective adaptation approach would be helpful to the users.

For color temperature conversion, experiments are performed on a MPEG-1 video clip (a length of 2108 frames) in accordance with the MPEG-21 DIA color temperature preference descriptor that is provided in Fig. 7; $CT_{\mathrm{Pref}} = \{(78, 100), (160, 178), (208, 185), (227, 205)\}$. Since this information can be interpreted that the user wants to emphasize the difference of color temperatures in low and high ranges, a sigmoidal function is utilized to construct a mapping function, as we addressed in Section III. If we approximate all preference points completely, the resulting function would increase very steeply in middle range and the differences of color temperatures in the middle range are emphasized too much. This is not desirable in color temperature conversion of continuous video sequence. Hence, the precision of approximation near (160, 178) is sacrificed as shown in Fig. 12.

Fig. 13 shows examples of temperature-converted frames of the video clip. The images with low temperature were converted so that their temperatures be lower as seen in Fig. 13(a) and (b). The images with relatively high temperature were converted so that their temperatures be higher as seen in Fig. 13(c)–(h). Fig. 14 shows the temporal trajectory of temperature mapping of all frames in the video clip. It is observed that the curve shapes of original (input) temperature and target temperature are very similar to each other, and the scale of temperature mapping is dependent upon each original temperature, which implies that the relative differences of color temperature between frames were effectively preserved. It should also be noted that the temperature of each converted image is almost same as the target temperature. It shows that the methods for color temperature estimation and conversion are consistent to each other and reliable, so that converted images have the preferred temperature of the user as intended.

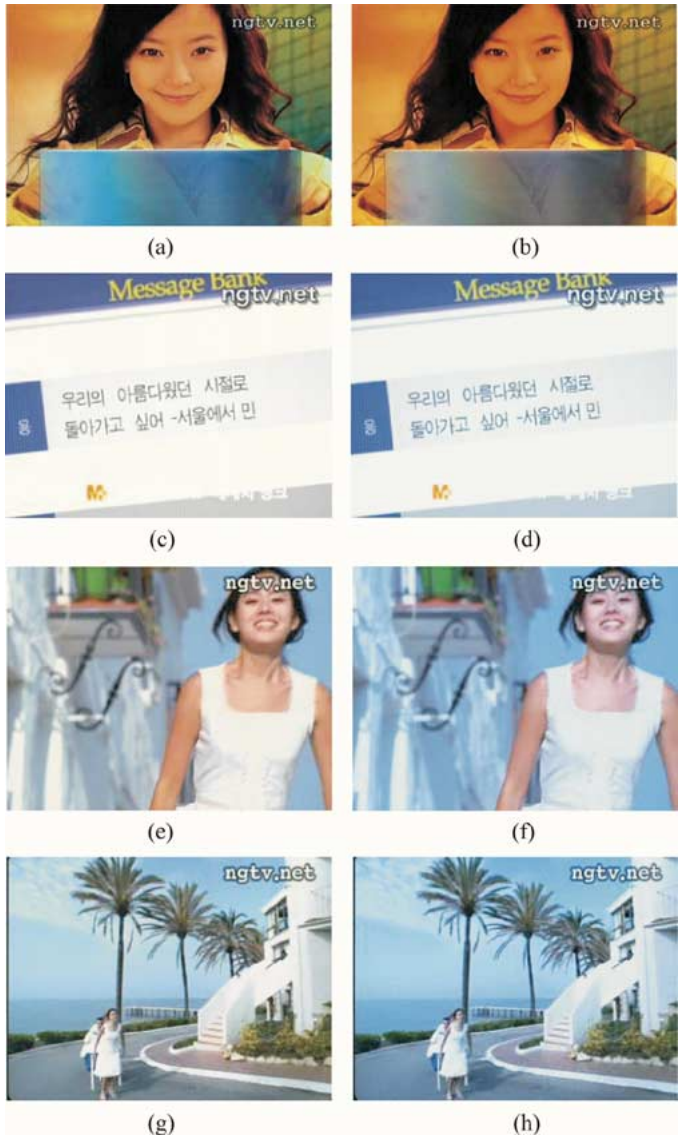

Fig. 13. Results of color temperature conversion: (a) original frame#1876; (b) converted frame#1876; (c) original frame#1928; (d) converted frame#1928; (e) original frame#745; (f) converted frame#745; (g) original frame#462; and (h) converted frame#462.

V. Conclusions

In this paper, we presented several adaptation techniques and experimental results for tailoring visual contents in accordance with user perception characteristics within the MPEG-21 DIA framework. Specifically, we addressed the modeling of conditions and adapting content for anomalous trichromacy and for combined low-vision symptoms. We provided experimental results based on clinical tests of color vision deficiency. We also

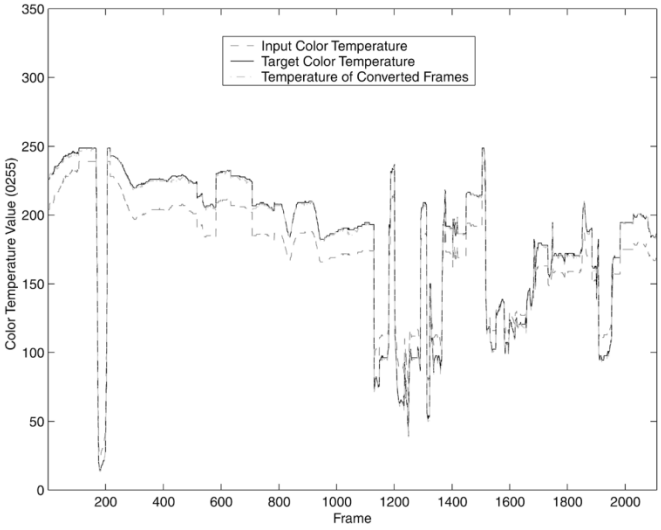

Fig. 14. Color temperature mapping.

presented experiments addressing color temperature adaptation using a temperature mapping scheme.

The issues of content adaptation based on user characteristics addressed in this paper are only part of larger MPEG-21 DIA standard. We anticipate that further work is required to harmonize and trade-off the multiple aspects of user characteristics, terminals and networks in the underlying various usage environment, to achieve the optimal perceived QoS in the personalized UMA services.

ACKNOWLEDGMENT

The authors would like to thank S. Yang and T. C. Thang at ICU for their helps and valuable suggestions, and Dr. J. H. Lee at SNUH and Dr. E. K. Wong at University of California, Irvine, for clinical experiments and advice. The authors also appreciate Dr. G. B. Beretta at Hewlett Packard Laboratories for his helpful comments and advice during MPEG-21 DIA standardization activities. They also thank the Associate Editor, Dr. J. R. Smith, and the anonymous reviewers of this paper for their helpful comments.

REFERENCES

[1] R. Mohan, J. R. Smith, and C.-S. Li, "Adapting multimedia internet content for universal access," *IEEE Trans. Multimedia*, vol. 1, no. 2, pp. 104–114, Mar. 1999.

[2] A. Vetro, C. Christopoulos, and T. Ebrahimi, *IEEE Signal Process. Mag.—Special Issue on Universal Multimedia Access (UMA)*, vol. 20, no. 2, Mar. 2003.

[3] I. Burnett, R. V. de Walle, K. Hill, J. Bormans, and F. Pereira, "MPEG-21: Goals and achievement," *IEEE Multimedia Mag.*, vol. 10, no. 4, pp. 60–70, 2003.

[4] B. L. Tseng, C.-Y. Lin, and J. R. Smith, "Using MPEG-7 and MPEG-21 for personalizing video," *IEEE Multimedia Mag.*, vol. 10, no. 4, pp. 42–52, 2003.

[5] P. van Beek, J. R. Smith, T. Ebrahimi, T. Suzuki, and J. Askelof, "Metadata-driven multimedia access," *IEEE Signal Process. Mag.*, vol. 20, no. 2, pp. 40–52, Mar. 2003.

[6] Information Technology, "Multimedia Content Description Interface—Part 5: Multimedia Description Schemes,", ISO/IEC 15938-5, 2002.

[7] Information Technology, "Multimedia Framework—Part 7: Digital Item Adaptation,", ISO/IEC 21000-7, 2004.

[8] W3C Recommendation. (1999) Web Content Accessibility Guidelines 1.0. [Online]. Available: http://www.w3.org/TR/WCAG10/

[9] C. Rigden, "The eye of the beholder designing for color-blind users," *British Telecommun. Eng.*, vol. 17, pp. 291–295, Jan. 1999.

[10] H. Brettel and F. Vienot, "Color display for dichromats," *Proc. SPIE, Color Imaging*, vol. 4300, pp. 199–207, 2001.

[11] G. Kovacs, I. Kucsera, G. Abraham, and K. Wenzel, "Enhancing color representation for anomalous trichromats on CRT monitors," *J. Color Res. Applicat.*, vol. 26, pp. 273–276, 2001.

[12] D. McIntyre, *Color Blindness: Cause and Effect*. Austin, TX: Dalton Publishing, 2002.

[13] V. C. Smith and J. Pokorny, "Spectral sensitivity of the fovea cone pigments between 400 and 700 nm," *Vis. Res.*, vol. 15, pp. 161–171, Feb. 1975.

[14] J. Nathans *et al.*, "Red, green, and red-green hybrid photopigments in the human retina: Correlations between deduced protein sequences and psychophysically measured spectral sensitivities," *J. Neurosci.*, vol. 18, pp. 10 053–10 069, 1998.

[15] J. Pokorny and V. C. Smith, "Evaluation of single-pigment shift model of anomalous trichromacy," *J. Opt. Soc. Amer.*, vol. 67, no. 9, pp. 1196–1209, Sep. 1977.

[16] I. Hardy, G. Rand, and C. Rittle, "HRR poly-chromatic plates," *J. Opt. Soc. Amer.*, vol. 44, pp. 509–523, 1954.

[17] D. Farnsworth, *The Farnsworth-Munsell 100-Hue Test for the Examination of Color Discrimination: Manual*. Baltimore, MD: Munsell Color Co..

[18] Y. M. Ro and S. Yang, "Color adaptation for anomalous trichromats," *Int. J. Imaging Syst. Technol.*, vol. 14, pp. 16–20, 2004.

[19] S. Yang and Y. M. Ro, "Visual contents adaptation for color vision deficiency," *Proc. IEEE ICIP*, vol. 1, pp. 453–456, Sep. 2003.

[20] J. Walraven and J. W. Alferdinck, "Color displays for the color blind," in *Proc. Color Science, Systems, and Applications of 5th Color Image Conf.*, 1997, pp. 17–22.

[21] American Foundation for the Blind. Blindness and low vision. [Online]. Available: http://www.afb.org

[22] Lighthouse International. Low vision defined. [Online]. Available: http://www.lighthouse.org/low_vision_defined.htm

[23] J. Nam *et al.*, "Report of CE on Visual Impairment,", Shanghai, China, ISO/IEC JTC1/SC29/WG11 M8958, 2002.

[24] E. Peli and T. Peli, "Image enhancement for the visually impaired," *Opt. Eng.*, vol. 23, pp. 47–51, 1984.

[25] P. Lennie and S. B. Van Hemel, *Visual Impairments: Determining Eligibility for Social Security Benefits*. Washington, DC: National Academy Press, 2002.

[26] M. Onoda and T. Harada, "2D filter design for the restoration of visually sharp images based on human perception characteristics," in *Proc. IEEE APCCAS 1998*, 1998, pp. 93–96.

[27] T.-L. Ji, M. K. Sundareshan, and H. Roehrig, "Adaptive image contrast enhancement based on human visual properties," *IEEE Trans. Med. Imag.*, vol. 13, no. 4, pp. 573–586, Dec. 1994.

[28] J. Ferwerda, S. N. Pattanaik, P. Shirley, and D. P. Greenberg, "A model of visual adaptation for realistic image synthesis," in *Proc. SIGGRAPH'96*, 1996, pp. 249–258.

[29] M. D. Fairchild, *Color Appearance Models*. Reading, MA: Addison-Wesley, 1997.

[30] R. Robertson, "Computation of correlated color temperature and distribution temperature," *J. Opt. Soc. Amer.*, vol. 58, no. 11, Nov. 1968.

[31] Visual extensions, "ISO/IEC 15938-3:2002/Amd 1:2004,", 2004.

[32] "Extensions of extraction and use of MPEG-7 descriptions, ISO/IEC TR 15938-8:2002/Amd 1:2004, 2004.,", 2004.

[33] D.-S. Park *et al.*, "User-preferred color temperature conversion for video on TV or PC," *Proc. IS&T/SPIE, Color Imag. VIII*, vol. 5008, pp. 285–293, Jan. 2003.

[34] S. Süsstrunk, J. Holm, and G. D. Finlayson, "Chromatic adaptation performance of different RGB sensors," *Proc. SPIE Electron. Imag. 2001*, vol. 4300, Jan. 2001.

[35] S. Yang *et al.*, "Report on CE for visual accessibility - Part 1: color vision deficiency,", Klagenfurt, Austria, ISO/IEC JTC1/SC29/WG11 M8543, 2002.

[36] M. S. Kim *et al.*, "Seohan computerized hue test: The development of computerized color vision test and pilot study," *J. Korean Ophthalmol. Soc.*, vol. 41, no. 1, 2000.

Jeho Nam (M'00) received the B.S. degree in electrical and control engineering from Hongik University, Seoul, Korea, in 1992 and the M.S. and Ph.D. degrees in electrical and computer engineering from the University of Minnesota, Minneapolis, in 1996 and 2000, respectively.

He is currently a Senior Member of the Engineering Staff at the Broadcasting Media Research Group, Electronics and Telecommunications Research Institute (ETRI), Daejeon, Korea. He has participated in standardization activities, including MPEG-7, MPEG-21, and TV-Anytime Forum. His research interests are in the areas of signal processing for digital video technologies and multimedia applications, in particular content-based audio/visual analysis, context-aware media adaptation, multimedia security and protection.

Dr. Nam is a member of ACM.

Yong Man Ro received the B.S. degree from the Department of Electronics Engineering, Yonsei University, Seoul, Korea, in 1985 and the M.S. and Ph.D. degrees from the Department of Electrical Engineering, Korea Advanced Institute of Science and Technology (KAIST), in 1987 and 1992, respectively.

He was a Researcher at Columbia University, New York, in 1987 to 1988, a Visiting Researcher at the University of California at Irvine and KAIST from 1992 to 1995, and a Research Fellow in the Department of Electrical Engineering and Computer Sciences, University of California at Berkeley, in 1996. He was also a Professor in the Department of Computer Engineering, Taejon University, until 1996. Since 1997, he has been with the Information and Communications University (ICU), Korea, where he is currently an Associate Professor of the Multimedia Communication Group and the director of IVY (Image/Video System) Lab. He participated in international standardizations including MPEG-7 and MPEG-21, where he contributed several MPEG-7 and MPEG-21 standardization works. His current research interests include multimedia adaptation/modality conversion, multimedia information retrieval, medical image processing and watermarking.

Dr. Ro received the Young Investigator Finalist Award of ISMRM in 1992 and the Scientist Award (Korea) in 2003. He was a Co-Program Chair of IWDW 2004.

Youngsik Huh received the B.S., M.S., and Ph.D. degrees from Korea Advanced Institute of Science and Technology, Daejeon, Korea, in 1993, 1995, and 2000, respectively, all in mathematics.

In 2000, he joined the Corporate Research Center, Samsung Electronics, Korea. From 2001 to 2003, he was a Member of Technical Staff with the Multimedia Laboratory, Samsung Advanced Institute of Technology, Yongin, Korea, where he had been involved in several projects on automatic structuring of digital video, color reproduction, and their applications into consumer electronics. Also, he participated in MPEG-7 and MPEG-21 standardization activities. He is currently an Assistant Professor of Mathematics in School of Natural Sciences, Hanyang University, Seoul, Korea. His research is focused on geometric topology in mathematics, specifically, theory of knots, links, and spatial graphs. He is also interested in adaptation of structured multimedia resources.

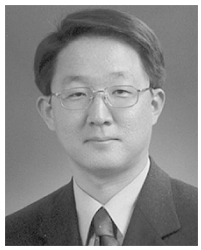

Munchurl Kim received the B.E. degree in electronics from Kyungpook National University, Korea, in 1989, and the M.E. and Ph.D. degrees in electrical and computer engineering from University of Florida, Gainesville, in 1992 and 1996, respectively.

He then joined the Electronics and Telecommunications Research Institute (ETRI), where he worked in the MPEG-4/7 standardization related research areas. Since 2000, he has been involved in the project management for the development of a data broadcasting end-to-end system for terrestrial digital broadcasting. In 2001, he joined the Information and Communications University (ICU), Daejeon, Korea, as an Assistant Professor of the School of Engineering. His research interesst include MPEG-4/7/21, video compression/communications, mobile multimedia broadcasting, intelligent and interactive multimedia, and pattern recognition.